Reaction ^{58}Ni(π^+,pp) at $T_{\pi^+} = 160$ MeV

W. J. Burger,[*] E. Beise,[†] S. Gilad,[‡] and R. P. Redwine
*Department of Physics and Laboratory for Nuclear Science, Massachusetts Institute of Technology,
Cambridge, Massachusetts 02139*

P. G. Roos, N. S. Chant, H. Breuer, G. Ciangaru,[§] and J. D. Silk[**]
Department of Physics and Astronomy, University of Maryland, College Park, Maryland 20742

G. S. Blanpied, B. M. Preedom, and B. G. Ritchie[††]
Department of Physics and Astronomy, University of South Carolina, Columbia, South Carolina 29208

M. Blecher and K. Gotow
Department of Physics, Virginia Polytechnic Institute and State University, Blacksburg, Virginia 24061

D. M. Lee and H. Ziock
Los Alamos National Laboratory, Los Alamos, New Mexico 87545
(Received 12 June 1989)

The reaction ^{58}Ni(π^+,pp) was studied with good energy resolution for an incident pion energy of 160 MeV. The angular correlation of the outgoing protons was measured for $\theta_{\text{lab}} = 30°$, 75°, and 130°. From these angular correlations the contribution from direct two-nucleon absorption was extracted. A Monte Carlo calculation modeling the absorption process in terms of initial-state scattering of the pion before absorption, two-nucleon absorption, and final-state scattering of the outgoing nucleons is compared to the data. We conclude that within this framework the two-nucleon mechanism can account for less than half of the total absorption cross section in ^{58}Ni. We report results for the low-energy coincidence proton spectra (down to 5 MeV) which suggest that most of these protons come from evaporation. Angular correlation data for the reaction ^{58}Ni(π^-,pp) are also presented.

I. INTRODUCTION

Pion absorption remains the focus of much attention in intermediate energy nuclear physics. In the last several years various groups have reported results from which a number of important questions have emerged. The investigations reported here are intended to address some of the central issues.

Pion absorption is an important reaction channel representing as much as ~30–40% of the total π-nucleus cross section in the $\Delta(1232)$ resonance region.[1] Consequently, its effects must be incorporated in models aimed at a description of π-nuclear phenomena. These effects may be introduced in various ways, e.g., via the imaginary part of the π-nucleus potential in a nuclear optical model,[2] or through the spreading potential used to describe the propagation of the Δ in Δ-hole model calculations.[3] Although such treatments may adequately reflect the effects of the absorption channel on the specific process studied, e.g., pion elastic scattering, they offer limited information on the details of the absorption mechanism itself.

Much of the past work in the area of pion absorption has concentrated on a two-nucleon absorption process in which the pion's energy and momentum are transferred to a nucleon pair in the target. Due to the large momentum mismatch between the initial and final states, absorption on a single nucleon within the nucleus is greatly suppressed; hence, the two-nucleon picture is the simplest and has as its free counterpart the deuteron. Several calculations exist which are based upon two-nucleon absorption in nuclei.[4] Further refinements are added to take into account pion scattering prior to absorption [initial-state interactions (ISI)] and scattering of the outgoing nucleus [final-state interactions (FSI)]. These calculations do a fair job of reproducing the absorption cross sections and some features of the data, but they have limited predictive power regarding details of the process, as we shall see.

Experimentally, there exist results from a number of studies[5] which have investigated nuclear absorption near the kinematics corresponding to the free two-nucleon process, i.e., quasideuteron absorption. These experiments typically report a clear signature from this mechanism in the data; however, other results suggest that the two-nucleon mechanism may not play a dominant role.

In particular, the inclusive measurement of McKeown et al.[6] has been cited as evidence for a multinucleon mechanism, i.e., one involving more than two nucleons in the absorption process. This group measured the inclusive reactions $(\pi^\pm,p)$ with various nuclear targets and incident pion energies. They obtained a ratio of ~4 for

the relative yield of protons from π^+/π^-, in contrast to the larger values (> 10) expected from spin-isospin considerations of two-nucleon absorption proceeding via the formation of an intermediate Δ-N state; a smaller ratio is consistent with participation of more than two nucleons in the reaction. It was concluded from a rapidity analysis of the same data that on average ~ 4 nucleons were involved.[7]

Girija and Kóltun[8] were able to reproduce the observed rapidities within the framework of a transport-type calculation by considering only absorption on nucleon pairs and by invoking a strong contribution from ISI. Subsequently, Tacik *et al.*[9] searched for such effects with an arrangement designed to detect the protons arising from quasifree πp scattering followed by absorption on an np pair to produce the reaction $^{12}C(\pi^+,ppp)$. The data did not reveal a clear signature for the two-step process.

A coincidence measurement of both outgoing protons represents a more detailed and direct method with which to study the reaction mechanism. In this way, Altman *et al.*[10] have estimated the contribution from direct two-nucleon absorption via an analysis of the angular correlation spectra of the (π^+,pp) reaction. They report that the direct two-nucleon component, as extracted from the data, represents $\sim 9\%$ of the total absorption cross section for ^{12}C near resonance, decreasing in importance to $\sim 2\%$ in the case of Bi. After correcting for FSI, these numbers rise to $\sim 20\%$. Representing as they do the total contributions from two-nucleon absorption, these values are remarkably small.

A second group, Wharton *et al.*,[11] has reported cross sections for transitions to the ^{14}N 1^+ ground state (g.s.) and 1^+ 4-MeV state in the reaction $^{16}O(\pi^+,pp)^{14}N$. For this quite restricted region where the quasideuteron mechanism dominates, Wharton *et al.* quote a combined cross section for the two 1^+ states which represents $\sim 7\%$ of the total absorption cross section. Their result is not inconsistent with the data of Altman *et al.*, bearing in mind that a significant extrapolation was required over the unmeasured portions of phase space.

Results from (π^+,pp) studies, particularly those of Altman *et al.*, have provoked much discussion, most of it related to the difficulty of reliably separating in such coincidence data the two-nucleon component from more complicated processes, i.e., ISI, FSI, and possible multinucleon absorption mechanisms. For example, Ritchie *et al.*[12] claim that in the case of ^{12}C, the analysis may underestimate the role of the two-nucleon mechanism. They employ a factorized distorted-wave impulse approximation (DWIA) to compute the expected angular correlation assuming absorption occurs in ^{12}C on a $1p$ shell np pair having either $L = 0$ or 2 orbital angular momentum with respect to the ^{10}B spectator core. It was found that the $L = 2$ component could contribute to that region of the angular correlation which Altman *et al.* had neglected as far as the possibility of containing an appreciable fraction of two-nucleon absorption events. Subsequently, a good energy resolution, wide acceptance measurement of the reaction $^{16}O(\pi^+,pp)$ at $T_\pi = 116$ MeV has been performed by Schumacher *et al.*[13] to further test the

DWIA approach. Their results indicate that at this lower energy the contribution from the two-nucleon mechanism, for the first 50 MeV of excitation of the residual nucleus, is approximately 40% of the total absorption cross section.

Our earlier published results[14] for the reaction $^{58}Ni(\pi^+,pp)$ were consistent with the general conclusion of Altman *et al.* In particular, we found that the region of the angular correlation identified with direct two-nucleon absorption was dominated by the low-excitation-energy region of the residual nucleus ($\leq$ 50-MeV excitation). The higher excitation region displayed little angular dependence, suggesting that more complicated processes were responsible. The direct two-nucleon yield extracted for Ni ($\sim 10\%$ of the absorption cross section) suggests a larger contribution from two-nucleon absorption than that extracted from the data of Altman *et al.*, though our conclusion regarding the relative importance of the non-two-nucleon mechanisms is similar.

There also exist coincidence data which may contain signatures of the ISI-FSI processes. Yokota *et al.*[15] have measured the (π^-,pp) reaction for ^6Li and C, reporting their results for 165-MeV incident energy. Two peaks are observed in the angular correlation data, the first in the forward-angle region and a second near the conjugate angle expected for two-nucleon absorption. The authors identify the forward-angle peak with proton-proton scattering following the (π^-,pn) reaction. The second peak is attributed to the (π°,pp) reaction following an initial-state charge-exchange scattering, $\pi^- p \rightarrow \pi^\circ n$. The two interpretations are supported by a comparison of the data to predictions of an intranuclear cascade model.[16] Unfortunately the authors do not attempt to estimate from their data the relative importance of such effects in the overall absorption process, though it appears to be small.

To summarize, though there now exist results from several experiments which indicate that a significant fraction of the absorption cross section lies outside the domain of the two-nucleon mechanism, the situation remains far from clear. The remaining uncertainties as to the specific influences of ISI and FSI in the two-nucleon channel have tended to make quantitative estimates of the multinucleon component difficult. Moreover, without a clear understanding of the role played by ISI-FSI, discussions of the reaction mechanism in terms of two-nucleon versus multinucleon processes are necessarily inconclusive. The situation is further obscured since possible alternate mechanisms are as yet unidentified. Much work, both theoretical and experimental, remains to be done.

We have previously presented part of our results[14] from the measurement of the reaction $^{58}Ni(\pi^+,pp)$. This paper provides additional details and reports the complete data set. The experiment emphasized energy resolution and dynamic range. In particular, the improved resolution (compared to previous wide acceptance studies) permitted an examination of the angular correlation spectra in terms of the ISI-two-nucleon-absorption-FSI scheme. The chosen detection angles enhanced our sensitivity to effects from ISI. We are therefore able to offer a

quantitative estimate of their role, and hence of the overall importance of the two-nucleon mechanism in pion absorption.

II. EXPERIMENTAL APPARATUS

The experiment was performed on the Low Energy Pion Channel (LEP) at the Clinton P. Anderson Meson Physics Facility (LAMPF) in Los Alamos, New Mexico.[17] A schematic view of the detector arrangement is shown in Fig. 1.

A. Beam

The beam channel was tuned to deliver 160-MeV positive pions within a momentum bite of 0.2–0.4%. The exact value was chosen to limit the counting rates in the NaI(Tl) detectors (described below). The beam position and profile were checked at the target position with a LAMPF-designed multiwire proportional chamber.[18] The profile monitor was later installed upstream of the target to provide a continuous check of the beam position and size during data taking. The final tune produced a

beam profile at the target of dimensions 2.4-cm FWHM horizontal (i.e., in the scattering plane), and 1.4-cm FWHM vertical.

The incident beam flux was monitored by several methods. A triple-detector telescope consisting of plastic scintillators with dimensions $5.08 \times 5.08 \times 0.318$ cm^3, $5.08 \times 5.08 \times 0.318$ cm^3, and $2.54 \times 2.54 \times 0.318$ cm^3, with each scintillator separated by 30.5 cm, was positioned 25.4 cm from the upstream window of the profile monitor at an angle of 120° with respect to the incident beam direction. The telescope detected incident particles scattered from the window of the profile monitor. In addition, an ionization chamber was placed downstream of the target to provide an integrated measure of the pion beam current. A toroid located on the primary proton beam line provided a similar measure of the proton flux incident on the carbon production target. The measurements from these three relative monitors agreed to within 6% throughout the experiment.

The absolute beam normalization was obtained by calibrating the relative monitors with a measurement of the ^{11}C activity[19] produced in the reaction ^{12}C(π^+,X)^{11}C. The average beam flux (typically 3.0×10^6/sec) was thus determined with a normalization uncertainty of $\sim 6.5\%$.

B. Targets and scattering chamber

Two isotopically enriched ($>95\%$) ^{58}Ni targets were used for the measurements. Most of the data was taken with a 218.7-mg/cm^2 thick, 7.5×5.0-cm^2 target. For an examination of the lowest-energy protons a 20.5-mg/cm^2, 5.08×5.08-cm^2 target was substituted. Calibration runs and checks required a third target, a 0.628-g/cm^2 thick, 6.23-cm-diam CD_2 disc.

The targets were mounted on a thin Al-frame ladder located inside a cylindrical Al scattering chamber, 30.5-cm high and 32 cm in diameter. A circular Al table was concentric with the chamber and served to support and position the NaI(Tl) telescopes. The scattering chamber vacuum reduced the energy loss the outgoing protons, especially important for the lowest-energy protons detected in Si surface barrier detectors located inside the chamber. The entire assembly was placed 1.7 m downstream of the last quadrupole magnet in the LEP channel.

FIG. 1. Schematic view of the experiment. In addition to the detector angles shown, the negative side counters were sometimes shifted by $-10°$ to provide more complete coverage of the angular correlation for the $+30°$, $+75°$, and $+130°$ angles.

C. NaI(Tl) detectors

Protons in the range 16–200 MeV were detected in an array of eight NaI(Tl) telescopes. These telescopes were positioned to provide reasonably good coverage of the in-plane angular correlation for $\theta_{lab} = +30°$, $+75°$, and $+130°$. Each telescope contained a $2.54 \times 2.54 \times 0.159$-cm^3 plastic scintillator followed by a $7.62 \times 7.62 \times 12.7$cm^3 NaI(Tl) crystal. The total thickness of the telescope was sufficient to stop protons with energies up to 200 MeV. The detected particles were identified by the combinations of energy deposited in the plastic scintillators (ΔE signal) and NaI(Tl) crystals (E signal). The solid angle subtended by each detector was typically 4.8 msr. The target-detector geometry eliminated problems of
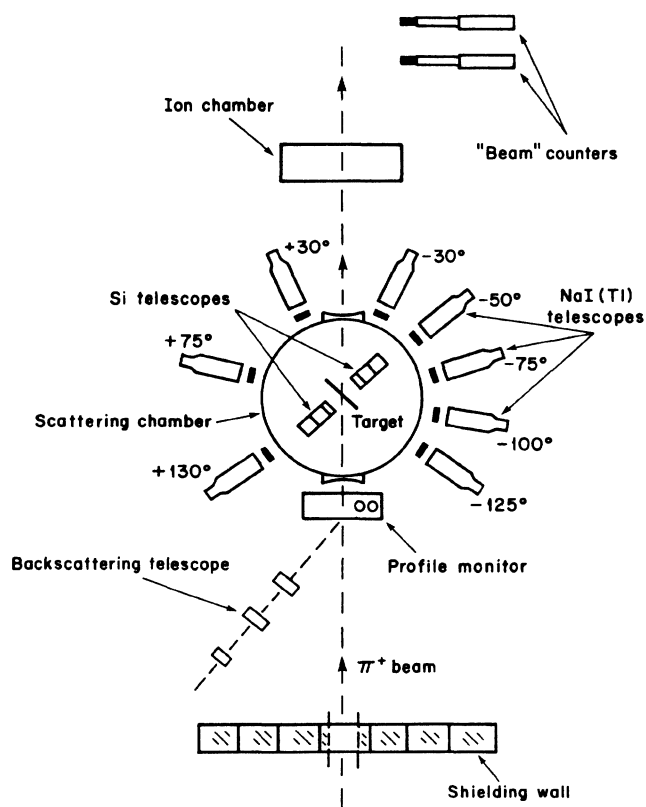
outscattering of protons in the detectors.

The telescopes were calibrated with protons from the reaction $\pi d \rightarrow pp$ using a CD_2 target and 160-MeV incident π^+'s. The resulting protons were detected at various angles and Al degraders were employed to obtain energies as low as 40 MeV. The energy resolution of an individual NaI(Tl) telescope was typically $\leq 5\%$ (FWHM) as determined from the energy calibration data. We estimate the resulting resolution for the coincidence data to be ~ 8 MeV in the missing mass.

The stability of the pulse height output of the NaI(Tl) detectors was monitored in several ways: light-emitting diode (LED) flashers, periodic CD_2 runs, and a check of the kinematic cutoffs present in the proton coincidence spectra (see Fig. 4 below). The gain corrections were $< 5\%$ in most cases.

D. Si detectors

Low-energy proton spectra were measured with a pair of Si surface barrier detector telescopes. Each of these telescopes consisted of a 1.27-cm thick brass collimator followed by a 50μ ΔE counter, a 1000μ E counter, and a 1000μ veto counter. The brass collimator had a 1.59-cm-diam circular aperture; the diameter of each Si counter was 3.25 cm. The dynamic range of the telescopes was 4–18 MeV taking into account energy losses in the target and including those protons stopping in the veto. The counters were calibrated by using previously determined energy-range relations.[20] The Si counters were positioned 45° out of the NaI(Tl) detection plane for angles of 60° and 120° with respect to the incident beam direction.

E. Computer and software

The on-line data acquisition software was the LAMPF "Q" package[21] which was used with a Digital Equipment Corporation PDP 11/45 computer. Off-line data replay and analysis were done with a modified version of "Q" running on a Digital VAX 11/780 machine.

The on-line system handled the multiple tasks of reading event data, writing events to tape, and distributing events to the PDP 11/45 for processing. The fast electronics were configured to trigger on events in which either a single telescope fired (prescaled), or > 1 telescope fired, the coincidence data. Additional triggers were defined to read out hardware scalars and to receive LED data. The deadtime for the system was typically 2–3 %.

III. DATA ANALYSIS AND RESULTS

Figure 2 shows a characteristic ΔE-E spectrum from one of the NaI(Tl) telescopes. Protons are seen to be separated from lighter mass particles, i.e., π's, μ's, and e's. The proton energies measured in the NaI(Tl) crystals were corrected for energy losses in the target, scattering chamber window, and plastic scintillators. The energy spectra were also adjusted to correct for protons reacting in the NaI(Tl), an effect as large as 25% for 200-MeV protons.[22]
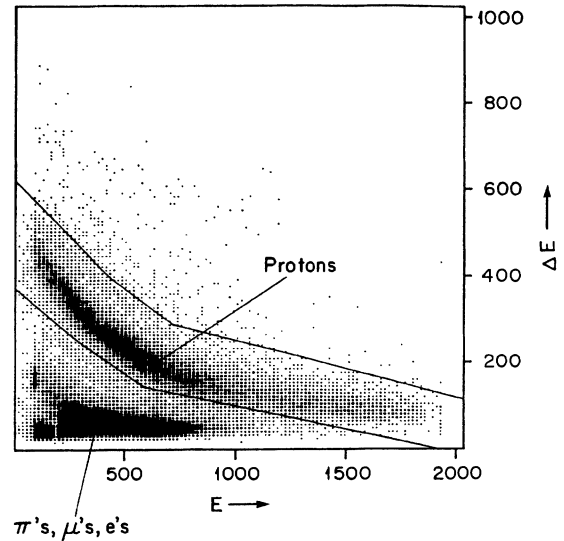
In order to apply this NaI(Tl) reaction correction to

FIG. 2. ΔE-E plot for the $-30°$ NaI(Tl) telescope. The solid lines indicate the proton cut that was used.

our continuous energy spectra, we have approximated as linear the shape of the reaction tail. The slope of the tail was defined by normalizing its area to the known tail-to-peak ratio,[22] subject to the condition that at zero energy the contribution is zero. For each energy spectrum, the correction algorithm started with the highest-energy bin, computed the tail-to-peak ratio, and then removed a fraction of this contribution from the lower-energy bins according to the above tail shape. The correction procedure proceeded from higher to lower energies incorporating the results from the higher-energy bins in subsequent steps. In the case of the coincidence data, each NaI(Tl) spectrum was corrected independently, thus ignoring the relatively rare events in which both protons reacted in the counters. Henceforth, all reference to the data will be understood to refer to the data corrected for reactions, as described above.

The error bars displayed with the data in the next sections reflect only the relative uncertainties in the quoted cross sections. These uncertainties were dominated by the uncertainties introduced by the particle identification cuts and by those of the detector acceptances. The former were typically 4% for the coincidence data and 6% for the singles data. For the most forward angles ($\pm 30°$) in the singles data, the uncertainty in particle identification was larger (~ 15–20 %) as a consequence of the higher counting rates recorded in those counters. The uncertainty in the detector acceptances ranged from 3–7 % for the NaI(Tl) telescopes and was 5% for the Si telescopes. The statistical uncertainties were small in comparison. An additional absolute uncertainty of 7% is assigned to the data (not shown in the figures), 6.5% from the beam normalization and 2% from the target thickness determinations.

A. (π^+,p) data

Figure 3 shows the inclusive proton spectra measured at three angles compared with similar data from

McKeown et al.[6] The two experiments are basically in agreement given the latter's quoted uncertainty in absolute normalization of 15%. A significant discrepancy between the two data sets is observed in the upper kinetic energy range ($T_p > 150$ MeV), particularly at backward angles. This difference may be explained in part by the smaller dynamic range of our NaI(Tl) crystals possibly resulting in a misidentification of those protons not stopped in the detectors. For the coincidence data the effects from such energetic protons are expected to be small, further minimized by the use of rather conservative energy cuts in the analysis.

The total angle-integrated proton yield for energies above 40 MeV was 1090 mb, 20% larger than the cross section reported by McKeown et al.

B. (π^+,pp) data

The proton coincidence data included events from all possible detector combinations, though the experimental setup emphasized those events near the kinematics of the two-body process. The coincident energy spectrum for one such pair located at the conjugate angles for quasideuteron absorption is displayed in Fig. 4. The data are seen to populated rather uniformly the region of physically allowed events, with some enhancement visible along the line corresponding to a small excitation of the residual nucleus. The events along the boundary are consistent with two-nucleon absorption modified primarily by the Fermi motion of the absorbing pair.

In an effort to determine the relative importance of the two-nucleon component, the angular correlation spectra were extracted with different cuts on the total detected energy. These cuts were (I) $T_{p1} + T_{p2} > 230$ MeV, including the first 50-MeV of excitation in the residual nucleus, (II) $T_{p1} + T_{p2} > 160$ MeV, the "guaranteed absorption cut," and (III) $T_{p1}, T_{p2} > 25$ MeV, representing the full range of our acceptance.

A clear signature of the two-nucleon component is seen in the energy spectrum of each arm of the ±75° coincidence pair. These are shown in Fig. 5 for the different cuts on the total detected energy. A broad peak is observed at the energy corresponding to two-nucleon absorption in each case except for that corresponding to the full total energy detection range.

Figure 6 shows the angular correlation for coincident protons detected at each of the laboratory angles
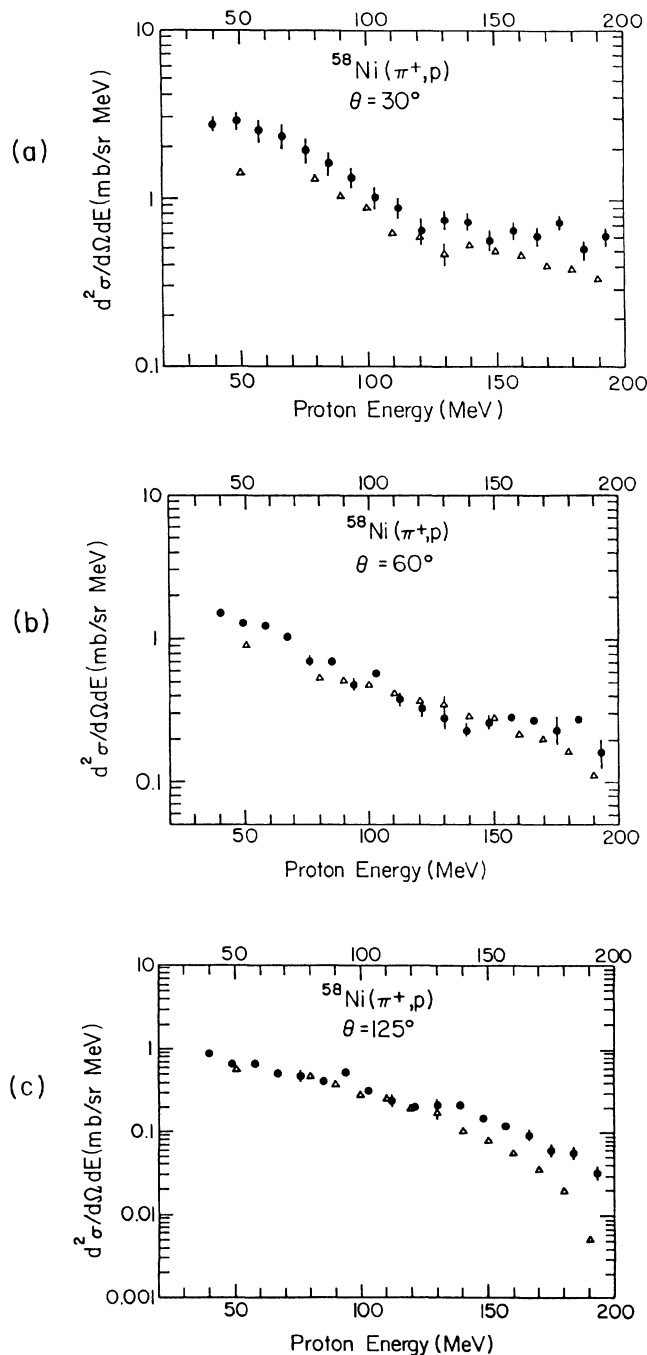

FIG. 3. (π^+,p) energy spectra. Data points represent ●, present experiment and △, data from McKeown et al. Ref. 6, for laboratory angles (a) 30°, (b) 60°, and (c) 125°.
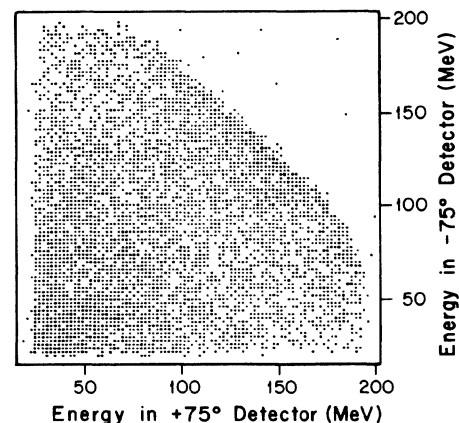
FIG. 4. E-E coincident energy distribution for the ±75° pair.

W. J. BURGER *et al.*

$\theta_{lab} = +30°$, $+75°$, and $+130°$ as well as our fits of the data with a function including two Gaussians. The widths and centroids of the Gaussians were unconstrained for the fits of the $+75°$ data of cuts I and II. For the $+75°$ data of cut III, the peak positions were constrained to be within $\pm 10°$ of the values resulting from

the cut I and cut II fits. In the case of the $+30°$ and $+130°$ distributions, the lack of data at extreme forward and backward angles required that the peak centroids be constrained to within $\pm 5°$ of the two-nucleon conjugate angle and that the widths be $\geq 20°$, in order to obtain a reasonable fit. We have chosen to perform the fits in the
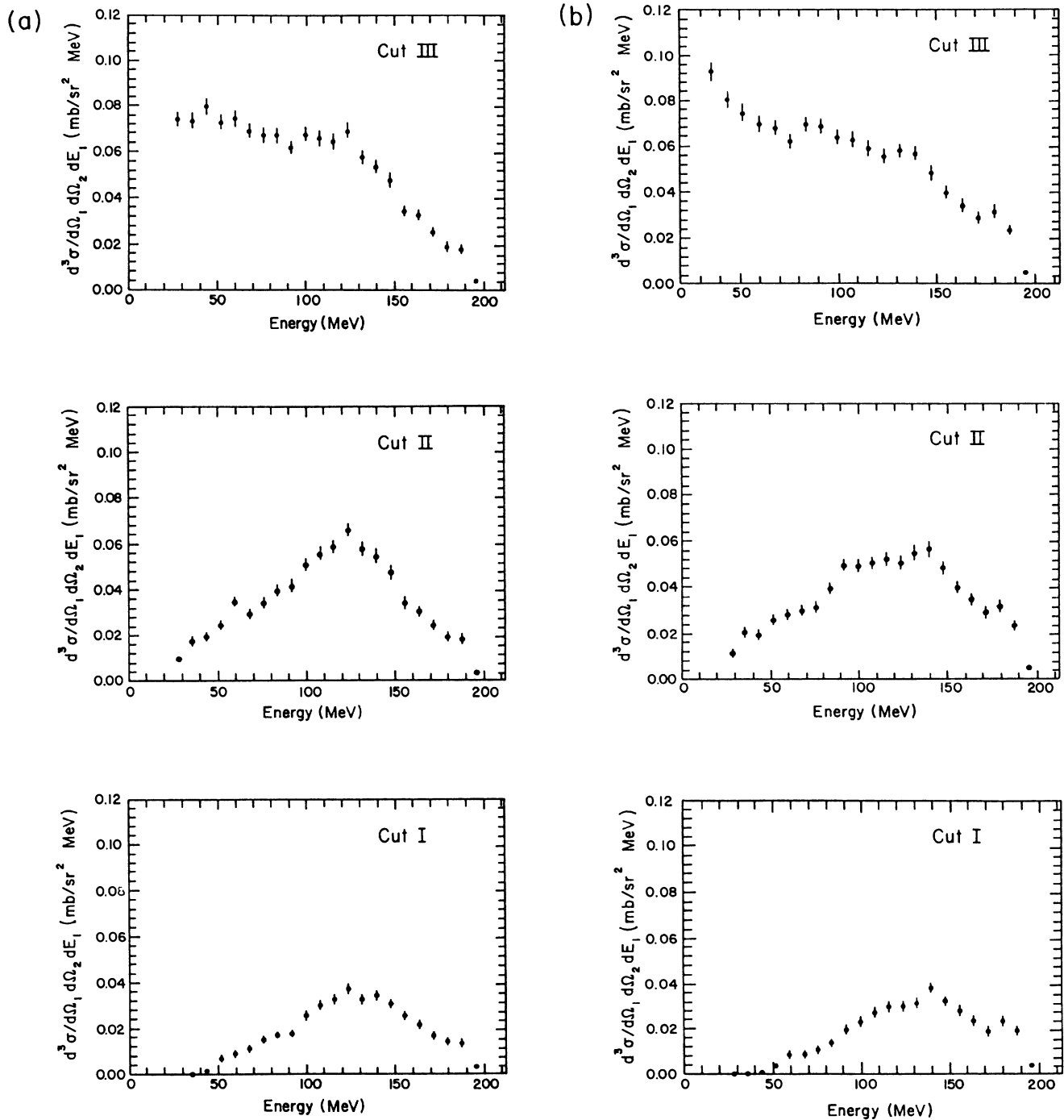

FIG. 5. Coincident energy spectra for (a) $-75°$ and (b) $+75°$ angle pair for the energy cuts I, II, and III described in the text.

π-NN center-of-momentum frame since the data appear more symmetrically distributed about the nominal two-body coincidence angle when analyzed in this frame. This choice would appear in any case to be the natural one for an examination of the two-nucleon mechanism.

A separate integration of each of the Gaussian regions yields the angular distributions shown in Fig. 7. In order to perform the solid angle integration, we have assumed the angular correlation out of the reaction plane to be

identical to that measured in plane for both Gaussian distributions. This assumption is consistent with previous measurements.[10] Although the number of angles is limited, the results for the narrow Gaussian are consistent with the angular distribution of the $\pi d \rightarrow pp$ reaction. Accordingly, to extract the cross section σ_{nar}, the angular distributions were fit with the standard Legendre polynomial parametrization of the $\pi d \rightarrow pp$ differential cross section.[23] For the broad Gaussian contribution which ap-
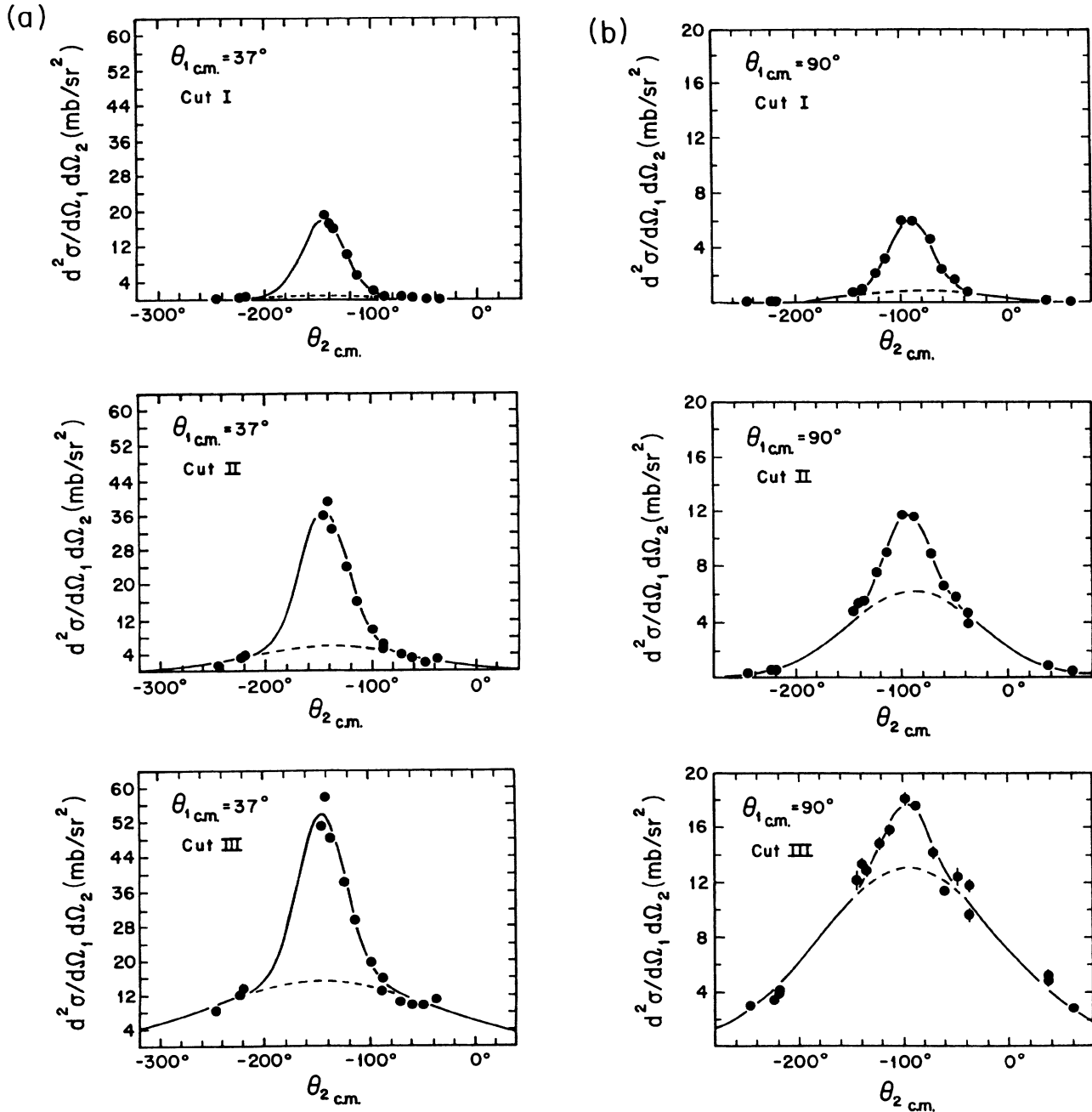

FIG. 6. The ^{58}Ni(π^+,pp) angular correlation for energy cuts I, II, and III (described in the text) for the laboratory angles (a) $+30°$, (b) $+75°$, and (c) $+130°$ (plotted in the πd center-of-momentum frame). The lines represent a two-Gaussian fit to the data.

pears to be independent of the angle $\theta_{c.m.1}$, the total cross section was obtained by multiplying the angle-averaged differential cross section by 2π. The results for both σ_{nar} and σ_{brd} are listed in Table I.

It is apparent from the distributions in Fig. 6 that the two-Gaussian fit is adequate to reproduce the observed angular correlation. Moreover, we believe this functional form serves to delineate the underlying physics, as evidenced by the good agreement between the narrow-

Gaussian angular distribution and the shape of the $\pi d \rightarrow pp$ reaction (noted earlier by Altman *et al.*[10]), and by the energy dependence of the Gaussians. The latter indicates that the events contributing to the narrow peak originate from relatively low excitations of the residual nucleus, precisely those events due to the direct two-nucleon mechanism. On the other hand, based on the observed flatness in the angular distribution associated with the broad Gaussian, there is evidence to suggest that
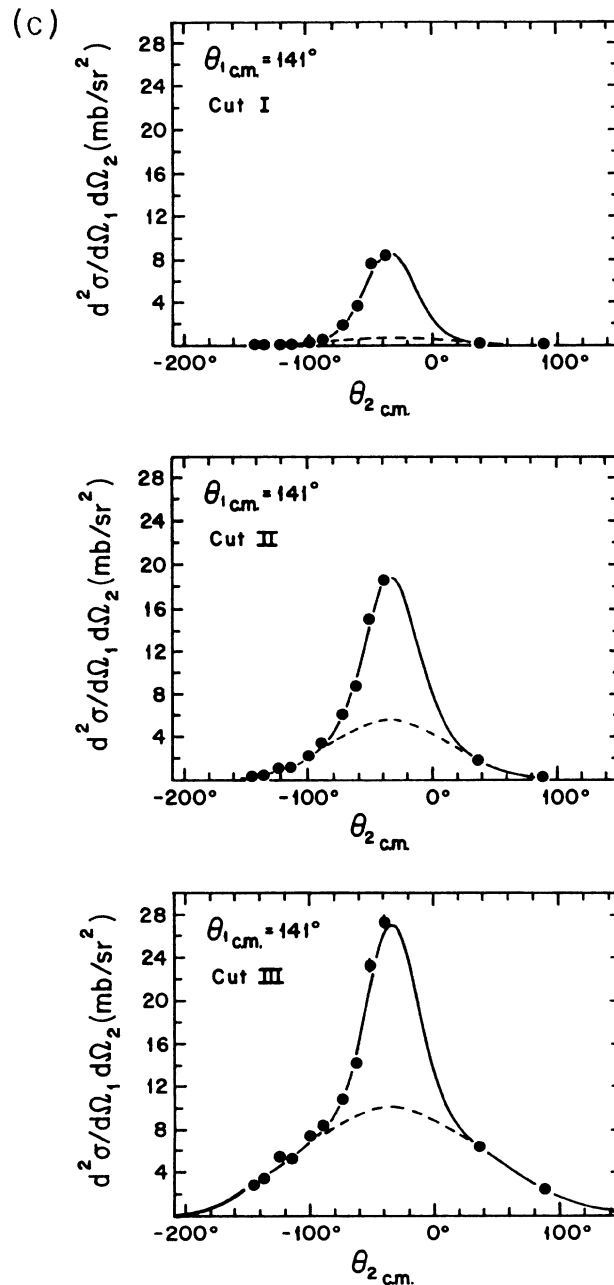

FIG. 6. *(Continued)*.

TABLE I. The ^{58}Ni(π^+,pp) cross sections σ_{nar} and σ_{brd} corresponding to the narrow and broad Gaussian components. The energy cuts are described in the text. Comparison is made to the total π^+-^{56}Fe absorption cross section σ_{abs} of Ref. 1. The listed uncertainties include those associated with the fitting procedure as well as the relative and absolute uncertainties described in the text. Since the sum of the narrow and broad Gaussians is better determined than each Gaussian alone, the listed uncertainties for $\sigma_{nar} + \sigma_{brd}$ might be considered to be conservative. However, a 7% uncertainty is included to reflect our assumptions concerning the shapes of the angular distributions.

Energy cut	σ_{nar} (mb)	$(d\sigma/d\Omega)_{brd}$ (mb/sr)	σ_{brd} (mb)	$\sigma_{nar} + \sigma_{brd}$ (mb)	$\sigma_{nar}/\sigma_{abs}$ (%)
I	41±5	2.6±0.5	16.6±3.0	58±6	7.0±1.3
II	55±8	26.8±3.5	168±22	223±23	9.5±2.0
III	53±14	88±9	555±58	608±60	9.2±2.8

most of the (π^+,pp) events are due to more complicated processes.

It may also be observed from Table I that for cut III the combined cross section of the narrow and broad peaks is consistent with the total Ni absorption cross sec-
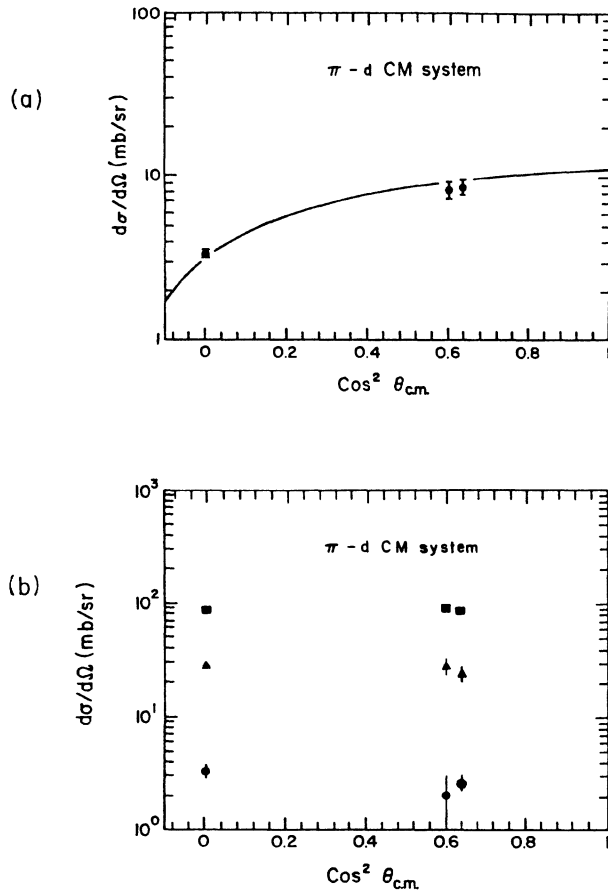

FIG. 7. (a) Angular distribution obtained from the narrow-Gaussian integration for cut I data. The solid line represents the $\pi d \rightarrow pp$ angular distribution fit to the data. (b) Angular distribution obtained from the broad Gaussian integration. The data points are ●, cut I; ▲, cut II; and ■, cut III.

tion. There are two significant effects which would cause our measured (π^+,pp) cross section to be different from the total absorption cross section, even assuming that the true (π^+,pp) cross section is representative of the total absorption cross section. First, events where the number of emitted protons is > 2 will cause us to overestimate the (π^+,pp) cross section. Second, our proton detection threshold of 16 MeV will cause us to underestimate the (π^+,pp) cross section. As these effects compensate to some extent, it may well be the case that almost every absorption event involves emission of at least two protons. However, at this point the agreement of our measured (π^+,pp) cross section with the total absorption cross section should be viewed as largely coincidental.

A more significant comparison is with similar quantities observed in other experiments. In Ref. 10, the total area of the two-Gaussian fit in ^{12}C corresponds to ~25% of the total absorption cross section. We have analyzed our data with an energy cut similar to those applied by Altman et al.[10] For this cut, we obtained a combined Gaussian contribution representing ~45% of the Ni absorption cross section. As one would expect to see a larger portion of σ_{abs} in the (π^+,pp) data for ^{12}C than for Ni, the experiments appear to be in disagreement. Also, when compared to the published results for Fe of Altman et al., our result for the direct two-nucleon component σ_{qd} is a factor of 2 larger.

C. (π^-,pp) data

We have also obtained a limited data set for the reaction ^{58}Ni(π^-,pp) representing a total incident pion flux ~15% of that used for the (π^-,pp) measurement. The angular correlations for the three angles +30°, +75°, and +130° are shown in Fig. 8. There appears to be an enhancement in the cross section near the conjugate angle of the two-nucleon process. Such events may be attributed to the two-step process consisting of an initial scattering $\pi^- p \rightarrow \pi^\circ n$ followed by absorption on a pp pair. This process has been suggested by the (π^-,pp) data of Yokota et al.[15] Our +30° and +75° data also show some indication of a second peak in the forward-angle region; such a peak, if present, could not be distinguished from the conjugate peak in the +130° data. The presence of a second peak at a forward angle would also be consistent with the data of Ref. 15.

The limited number of data points in Fig. 8 precludes a detailed analysis, thus we are not able to identify or offer estimates of the contributions of the separate ISI, FSI, or possible multinucleon absorption processes. However, since the events observed in the (π^-,pp) channel cannot arise solely from direct two-nucleon absorption, it is in-

TABLE II. The ^{58}Ni(π^-,pp) cross sections σ_{exp} for energy cuts II and III described in the text. The extracted cross sections are compared to the total $\pi^- $-^{56}Fe absorption cross section σ_{abs} of Ref. 1.

Energy cut	σ_{exp} (mb)	$\sigma_{exp}/\sigma_{abs}$ (%)
II	24.5±9.6	3.6±1.5
III	112.0±42.5	16.7±6.6

teresting to estimate its importance in relation to the total π^- absorption cross section. The measured cross sections for the previously defined energy cuts II and III are presented in Table II; for cut I the measured cross section was consistent with zero. In order to perform the solid angle integrations we have used constant angle-averaged values for the differential cross sections. The quoted errors are dominated by the 30% uncertainty assigned to this procedure.

D. Low-energy proton spectra

Before concluding with a further discussion of the (π^+,pp) data, we present data for the lowest-energy proton spectra (5–15 MeV). Previous $(\pi,2N)$ studies have largely ignored this energy region which nonetheless contains a large fraction of the protons resulting from absorption. Figure 9 shows the two-dimensional ΔE-E distribution for particles detected in the forward-angle Si telescope. Cleanly separated proton and deuteron bands may be identified.

Proton distributions representing our full detection range, 5–200 MeV, as shown in Fig. 10 for several different pairs of coincident angles. These spectra were
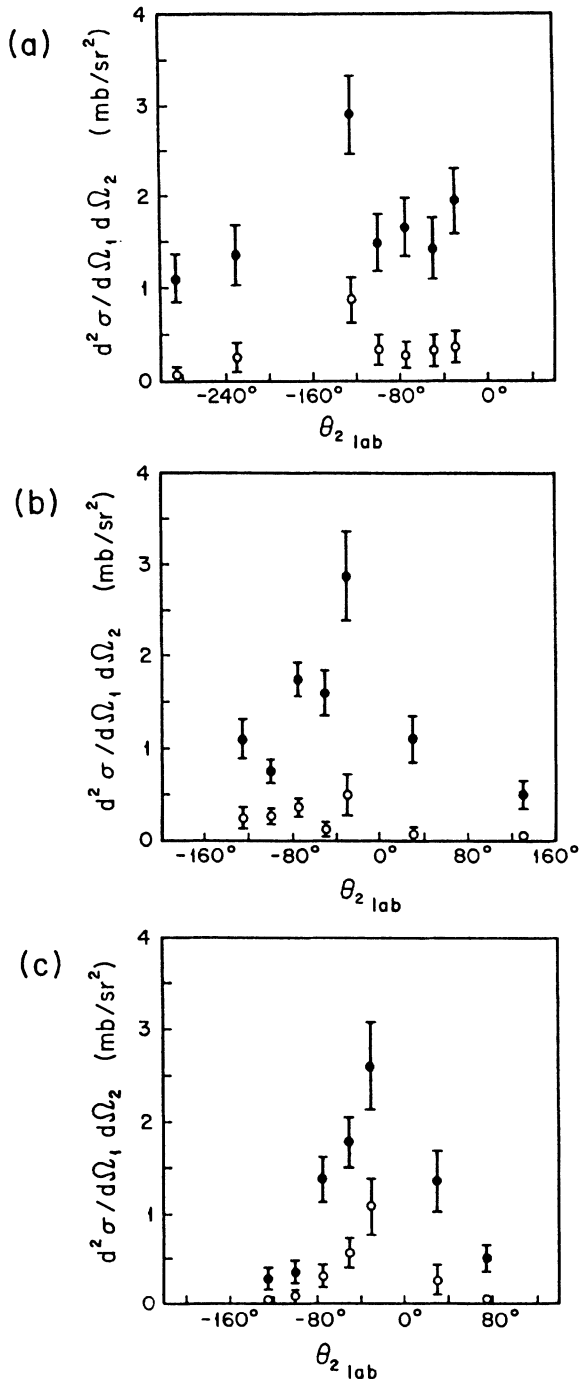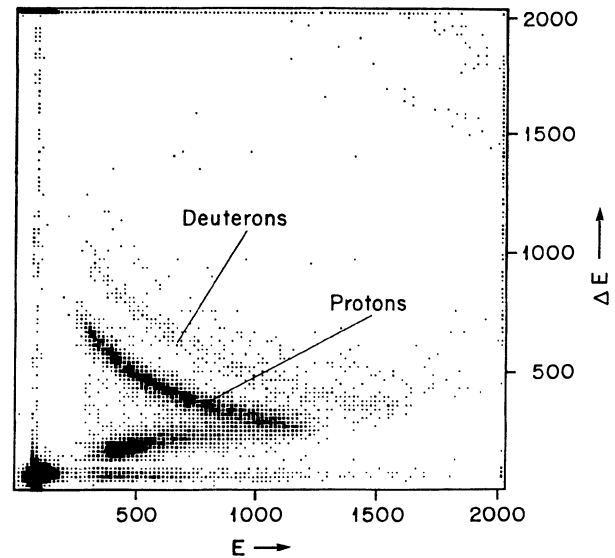
FIG. 8. The ^{58}Ni(π^-,pp) angular correlation for cuts II (○) and III (●) (described in the text) for the angles (a) +30°, (b) +75°, and (c) +130° plotted in the lab frame.

FIG. 9. ΔE-E spectrum from the forward-angle Si detector telescope.

constructed by plotting the lower-energy data of the −60° Si telescope with the data of either the −50° or −60° NaI(Tl) telescopes. The energies of the coincident protons detected in the NaI(Tl) counters were integrated over the full range of those counters, 16–200 MeV. The angles indicated for all counters were measured with respect to the incident beam direction.

A comparison of the different spectra reveals some differences at the highest proton energies. In particular, the data of Figs. 10(c) and 10(d) exhibit a sharper falloff with increasing proton energy. Such behavior can be understood in terms of two-nucleon absorption which dominates the upper end of the proton spectra, since these data correspond to opening angles farther away from the nominal opening angle of the two-nucleon process.

In the lowest-energy region, the data from the four detector pairs display similar behavior. Beginning at ~20 MeV, the spectra show a more rapid rise in cross section with decreasing energy, the cross section then appears to level off in the range 5–10 MeV. The shape of the distribution, particularly in the transition region 15–20 MeV, is quite similar to that reported for proton spectra obtained from (p,pp) and (p,p') reaction studies.[24] These lowest-energy protons from the proton-induced reactions have been identified as evaporation products with the peak of the evaporation spectra reported at ~5 MeV.[25]

We have estimated the proton yield below 20 MeV in the energy spectra of Fig. 10 by integrating over the angles θ_c [the coincident NaI(Tl) detector] and θ_s (the Si detector). The angular correlations as a function of θ_c were found to peak about the incident beam direction, which is consistent with the relatively higher probability for forward-angle protons to be produced in the reaction. The θ_c distribution was described by a simple function consisting of a Gaussian term centered at 0° and a flat constant term. In order to integrate over the second angle θ_s, we have assumed this distribution to be isotropic consistent with the view that this lowest-energy region is dominated by evaporation. The resulting total proton yield in the region 5–20 MeV is 654±100 mb, the uncertainty arising primarily from the uncertainties associated with the solid angle integrations. The rather large contribution reflects the dominance of the low-energy protons in the energy spectra.

An estimate of the deuteron content in the Si spectrum of Fig. 9 was also made. The corresponding deuteron angular distributions were quite similar to those of the pro-
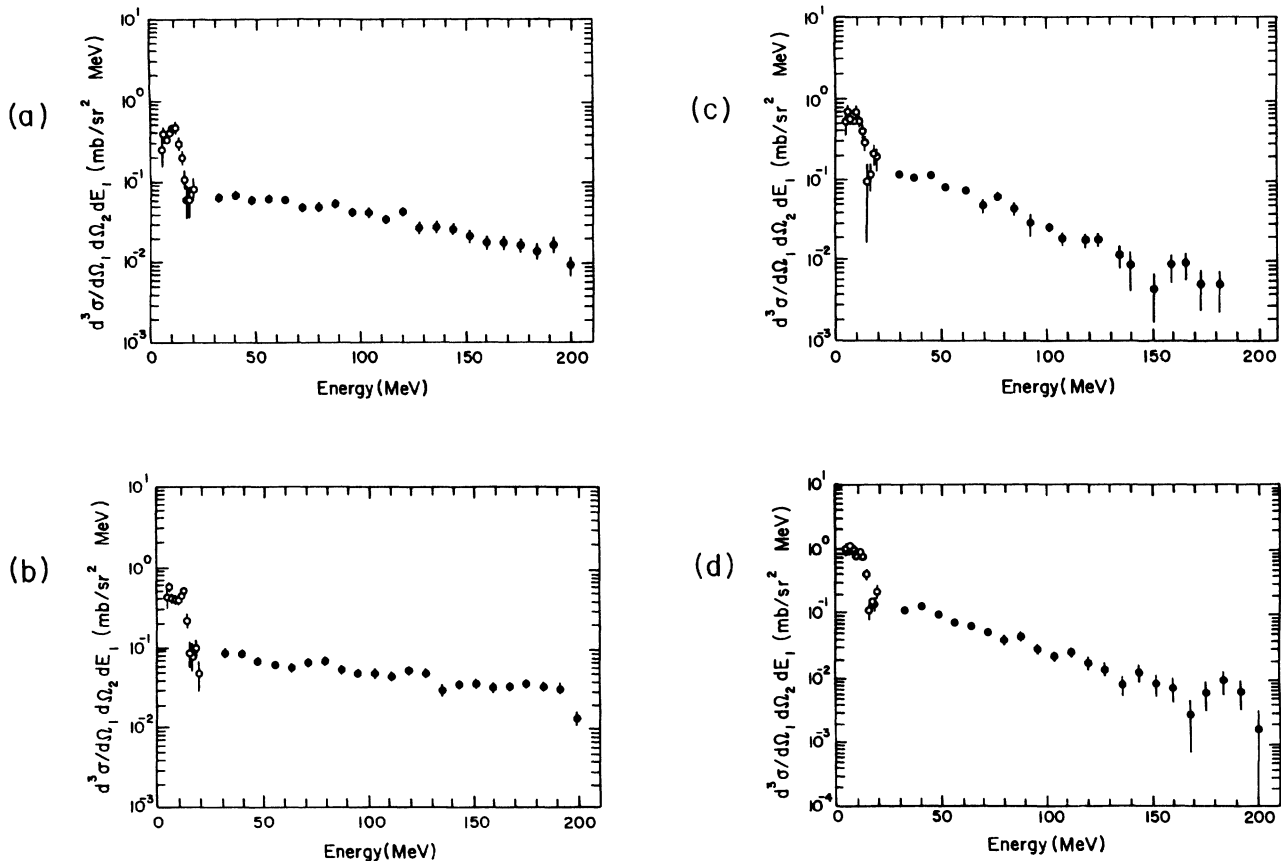

FIG. 10. Coincident proton energy spectra. Data below 20 MeV are from the 60° Si telescope. Data above 20 MeV are from either the 50° or 60° NaI(Tl) telescopes. Angles of coincident NaI(Tl) telescopes are (a) +130°, (b) +75°, (c) −125°, and (d) +30°.

ton spectra. Using an identical procedure to that applied to the proton distribution (including the assumption of an isotropic distribution for θ_s), we obtained a yield of 47 ± 8 mb for deuterons in the range 5–15 MeV. The resulting $p:d$ ratio was 15:1 within an uncertainty of 25%, which may be compared with the 30:1 ratio (20% uncertainty) obtained by Wu *et al.*[25]

IV. DISCUSSION AND CONCLUSIONS

In the above presentation of the (π^+,pp) data, it was claimed that the narrower-Gaussian events could be explained in terms of direct two-nucleon absorption. It is seen in Table I that the fraction of the absorption cross section in the narrow Gaussian (and thus associated with direct two-nucleon absorption) is independent of the energy cut, within the uncertainties of this experiment. We therefore take the somewhat conservative value of 10% as being representative of this fraction. There remain, however, questions concerning the possible importance of (π^+,pn) events, the roles played by ISI and FSI, and hence of the overall contribution of the (π^+,pp) mechanism to the π^+ absorption process in nuclei.

In regard to the (π^+,pn) reaction, there is considerable experimental information[26] indicating that absorption on isospin $T=1$ nucleon pairs is suppressed relative to absorption on $T=0$ pairs by at least an order of magnitude. These experiments compared the ${}^3\text{He}(\pi^+,pp)$ and ${}^3\text{He}(\pi^-,pn)$ reactions in quasifree kinematics. The observed suppression is understood qualitatively in terms of dominance of the ΔN intermediate channel.

The proposed role[8] of ISI in connection with the $(\pi^\pm,p)$ rapidity data was stated earlier. It has been pointed out that coincidence measurements of the outgoing nucleons should provide some sensitivity for observing such effects.[27] For example, the proton pair emerging at $\pm90°$ in the π-NN center-of-momentum frame corresponds to the minimum separation angle for protons observed in the lab. Consequently, effects from the scattering of the pion prior to absorption will result, on average, in events with larger separation angles. The $+75°$ angular correlation data shown in Fig. 6(b) correspond to the $\pm90°$ center-of-momentum pair for the kinematics of the present experiment.

A Monte Carlo calculation has been performed and compared to these angular correlation data. In the calculation, the reaction mechanism was modeled in terms of ISI, followed by absorption on a nucleon pair, followed by FSI. The specific FSI events considered here are "soft" events, in which the outgoing nucleon does not lose appreciable energy. The kinematics of each stage were defined by the corresponding free processes: $\pi N \rightarrow \pi N$, $\pi NN \rightarrow NN$, and $NN \rightarrow NN$. The momenta of the target nucleons were obtained from a zero-temperature Fermi gas distribution with $p_F = 270$ MeV/c, while the momentum of the absorbing nucleon pair was parametrized as a Gaussian distribution centered at zero momentum. The strength of the N-N interaction in the final state was chosen on the basis of estimates of the nucleon mean free path.[28]

The results of the calculation for no ISI are shown in

Fig. 11(a). The Monte Carlo distribution is compared with that part of the data previously identified as direct two-nucleon absorption, i.e., the data of cut I. With a FWHM of 300 MeV/c for the absorbing pair momentum distribution, the agreement is quite good. The measured angular correlation does appear to peak at a slightly larger separation angle consistent with some contribution from ISI. Note that the comparison between data and calculation is confined to the shape of the angular correlation; no attempt has been made to predict the magnitudes of the observed cross sections.
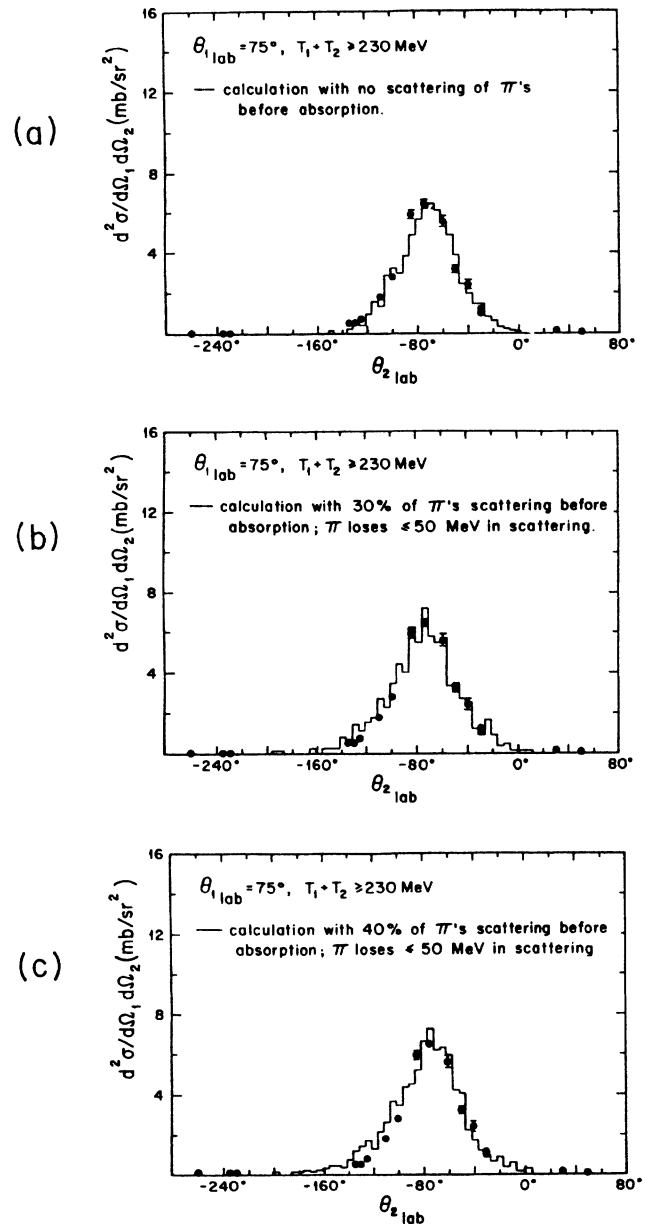

FIG. 11. Monte Carlo results (histogram normalized to the data) compared to the data of cut I for different fractions of the pions scattering before absorption: (a) no initial-state scattering, (b) 30%, and (c) 40% of the incident π's scattering before absorption.

In the next stage of the calculation, the percentage of incident pions participating in ISI was varied (each interacting pion presumed to undergo one such scattering). Figures 11(b) and 11(c) show the comparison with the Monte Carlo results for 30 and 40 % of the incident pions scattering. The data are consistent with ISI accompanying $\sim \frac{1}{3}$ of the events, a rather surprisingly small number in view of the strong πN interaction. It is also apparent that those events affected by initial-state scattering are for the most part confined to the narrower-Gaussian region (FWHM of 30°–40°). The same conclusion is supported by the (π^-,pp) data of Ref. 15 where the effects of ISI were observed to result in a $\sim 15°$ shift of the coincident proton peak from the nominal two-nucleon angle. In an estimation of the overall importance of the two-nucleon mechanism such ISI events would not augment the contribution extracted for the direct component. Furthermore, ISI at the level indicated by our comparison would be unable to explain the ($\pi^\pm$,p) rapidities via the mechanism proposed by Girija and Koltun.[8]

The influence of FSI is expected to be quite different. In particular, because protons will be scattered at large angles, events will be removed from the narrower peak region. These considerations lead to an increase of our two-nucleon estimate. Using a nucleon mean free path of 5 fm, and computing an average path length for the outgoing protons (~ 5.5 fm), by taking a weighted average of the path lengths for protons arising from absorption events occurring on the back surface of a spherical Ni nucleus, FSI would affect $\frac{2}{3}$ of the events. Therefore, the direct reaction component would be increased by a factor of 3, resulting in an estimated total contribution from two-nucleon absorption of $\sim 30\%$.

Clearly the final number is dependent on the input used for FSI. The nucleon mean free path λ itself has been the subject of discussion. Experimental values from a detailed analysis of elastic proton scattering[29] and the resonance behavior exhibited by total neutron cross sections[30] typically yield values ~ 5 fm, while a simple estimate based on nuclear densities and nucleon-nucleon cross sections predicts a λ of 1–2 fm. Subsequent progress[28] has been able to bring into agreement theoretical prediction and the larger experimental values. With a λ in the range 4–5 fm, it is difficult to account for most of the absorption cross section via the two-nucleon mechanism, given the small size of the direct component as extracted in our analysis.

However, it has been claimed that the two-Gaussian

analysis of the (π^+,pp) data, at least in ^{12}C, underestimates the role of the two-nucleon mechanism. In order to further test this suggestion, the DWIA calculation of Ref. 12 was repeated for Ni, including in the calculation all $f_{7/2}$ configurations with zero oscillator quanta in the n-p relative motion. At its present level of sophistication the DWIA approach failed to predict a two-nucleon component outside the region of the narrower Gaussian. Indeed, the calculation produced distributions a factor of 3 narrower, and a factor of 50 smaller than observed in the data.

While it appears that the point raised by Ritchie et al.[12] concerning absorption on $L > 0$ deuterons (angular momentum relative to the "spectator" nucleus) is a correct one, in our present case the stability of the extracted cross sections with respect to excitation energy cuts and shape of the resultant angular distributions lead us to conclude that the Gaussian analysis is adequate and produces the correct physics result. The ^{16}O(π^+,pp) results of Ref. 13 in fact provide support for the approach. While the good energy resolution allows one to see quite varied correlation shapes for low-lying states, depending on the specific angular momenta involved, the inclusion of events with excitation energies up to 50 MeV results in a narrow Gaussian with a width quite similar to that for our ^{58}Ni data. Furthermore, the area and width of that narrow Gaussian appear to be relatively independent of inclusion of events with greater residual excitation.

Therefore, we are led to conclude that $\sim 30\%$ of the absorption cross section in Ni originates from the two-nucleon mechanism. Initial-state scattering of the pion does not appear to be as significant as one may have expected. While it is true that events related to FSI populate the broader Gaussian, perhaps accounting for much of its overall shape, such events alone cannot account for the remaining absorption cross section. These observations lead us to conclude that the broad Gaussian component, which represents the major share of the (π^+,pp) cross section, contains a significant contribution from coherent processes involving more than two nucleons.

ACKNOWLEDGMENTS

---

*Present address: Paul Scherrer Institute, CH-5234 Villigen, Switzerland. Work address: CERN, EP Division, CH-1211 Geneva 23, Switzerland.

†Present address: California Institute of Technology, 425-48 Physics, Pasadena, CA 91125.

‡Present address: Scitex Corporation Ltd., 46103 Herzlia B, Israel.

§Present address: Schlumberger Well Services–Engineering, P.O. Box 4594, Houston, TX 77210.

**Present address: University of Pennsylvania, Philadelphia,

PA 19104.

††Present address: Arizona State University, Tempe, AZ 85287.

[1]D. Ashery, I. Navon, G. Azuelos, H. K. Walter, H. J. Pfeiffer, and F. W. Schlepütz, Phys. Rev. C 23, 2173 (1981).

[2]K. Stricker, H. McManus, and J. A. Carr, Phys. Rev. C 19, 929 (1979).

[3]M. Hirata, J. H. Koch, F. Lenz, and E. J. Moniz, Ann. Phys. (N.Y.) 120, 205 (1979).

[4]K. Masutani and K. Yazaki, Phys. Lett. 104B, 1 (1981); K.

Ohta, M. Thies, and T.-S. H. Lee, Ann. Phys. (N.Y.) **163**, 420 (1985).

[5]R. L. Burman and M. E. Nordberg, Jr., Phys. Rev. Lett. **21**, 229 (1968); J. Favier, T. Bressani, G. Charpak, L. Massonnet, W. E. Meyerhof, and C. Zupančić, Nucl. Phys. **A169**, 540 (1971); E. D. Arthur, W. C. Lam, J. Amato, D. Axen, R. L. Burman, P. Fessenden, R. Macek, J. Oostens, W. Shlaer, S. Sobottka, M. Salomon, and W. Swenson, Phys. Rev. C **11**, 3332 (1975).

[6]R. D. McKeown, S. J. Sanders, J. P. Schiffer, H. E. Jackson, M. Paul, J. R. Specht, E. J. Stephenson, R. P. Redwine, and R. E. Segel, Phys. Rev. C **24**, 211 (1981).

[7]R. D. McKeown, S. J. Sanders, J. P. Schiffer, H. E. Jackson, M. Paul, J. R. Specht, E. J. Stephenson, R. P. Redwine, and R. E. Segel, Phys. Rev. Lett. **44**, 1033 (1980).

[8]V. Girija and D. S. Koltun, Phys. Rev. C **31**, 2147 (1985).

[9]R. Tacik, E. T. Boschitz, W. Gyles, W. List, and C. R. Ottermann, Phys. Rev. C **32**, 1335 (1985).

[10]A. Altman, E. Piasetzky, J. Lichtenstadt, A. I. Yavin, D. Ashery, R. J. Powers, W. Bertl, L. Felawka, H. K. Walter, R. G. Winter, and J. v. d. Pluym, Phys. Rev. Lett. **50**, 1187 (1983); A. Altman, D. Ashery, E. Piasetzky, J. Lichtenstadt, A. I. Yavin, W. Bertl, L. Felawka, H. K. Walter, R. J. Powers, R. G. Winter, and J. v. d. Pluym, Phys. Rev. C **34**, 1757 (1986).

[11]W. R. Wharton, P. D. Barnes, B. Bassalleck, R. A. Eisenstein, G. Franklin, R. Grace, C. Maher, P. Pile, R. Rieder, J. Szymanski, J. R. Comfort, F. Takeutchi, J. F. Amann, S. A. Dytman, and K. G. R. Doss, Phys. Rev. C **31**, 526 (1985).

[12]B. G. Ritchie, N. S. Chant, and P. G. Roos, Phys. Rev. C **30**, 969 (1984); D. Ashery, *ibid.* **32**, 333 (1985).

[13]R. A. Schumacher, P. A. Amaudruz, C. H. Q. Ingram, U. Sennhauser, H. Breuer, N. S. Chant, A. E. Feldman, B. S. Flanders, F. Khazaie, D. J. Mack, P. G. Roos, J. D. Silk, and G. S. Kyle, Phys. Rev. C **38**, 2205 (1988).

[14]W. J. Burger, E. Beise, S. Gilad, R. P. Redwine, P. G. Roos, N. S. Chant, H. Breuer, G. Ciangaru, J. D. Silk, G. S. Blanpied, B. M. Preedom, B. G. Ritchie, M. Blecher, K. Gotow, D. M. Lee, and H. Ziock, Phys. Rev. Lett. **57**, 58 (1986).

[15]H. Yokota, T. Mori, T. Katsumi, S. Igarashi, K. Hama, R. Chiba, K. Nakai, J. Chiba, H. En'yo, S. Sasaki, T. Nagae, and M. Sekimoto, Phys. Rev. Lett. **58**, 191 (1987).

[16]Z. Fraenkel, E. Piasetzky, and G. Kalbermann, Phys. Rev. C **26**, 1618 (1982).

[17]R. L. Burman, R. L. Fulton, and M. Jakobson, Nucl. Instrum.

Methods **131**, 29 (1975).

[18]G. J. Krause and P. A. M. Gram, Nucl. Instrum. Methods **156**, 365 (1978).

[19]B. J. Dropesky, G. W. Butler, C. J. Orth, R. A. Williams, M. A. Yates-Williams, G. Friedlander, and S. B. Kaufman, Phys. Rev. C **20**, 1844 (1979); G. W. Butler, B. J. Dropesky, C. J. Orth, R. E. L. Green, R. G. Korteling, and G. K. Y. Lam, *ibid.* **26**, 1737 (1982).

[20]J. F. Janni, Kirtland Air Force Base Technical Report AFWL-TR-65-150, 1966.

[21]LAMPF Internal Report MP-1-3401-3, 1982.

[22]A. Bracco, H. P. Gubler, D. K. Hasell, W. T. H. van Oers, R. Abegg, C. A. Miller, M. B. Epstein, D. A. Krausse, D. J. Margaziota, and A. W. Stetz, Nucl. Instrum. Methods **219**, 329 (1984).

[23]C. Richard-Serre, W. Hirt, D. F. Measday, E. G. Michaelis, M. J. M. Saltmarsh, and P. Skarek, Nucl. Phys. **B20**, 413 (1970).

[24]A. A. Cowley, C. C. Chang, H. D. Holmgren, J. D. Silk, D. L. Hendrie, R. W. Koontz, P. G. Roos, C. Samanta, and J. R. Wu, Phys. Rev. Lett. **45**, 1930 (1980).

[25]J. R. Wu, C. C. Chang, H. D. Holmgren, Phys. Rev. C **19**, 698 (1979).

[26]D. Ashery, R. J. Holtz, H. E. Jackson, J. P. Schiffer, J. R. Specht, K. E. Stephenson, R. D. McKeown, J. Ungar, R. E. Segel, and P. Zupranski, Phys. Rev. Lett. **47**, 895 (1981); P. Gotta, M. Dörr, W. Fetscher, G. Schmidt, H. Ullrich, G. Backenstoss, W. Kowald, I. Schwanner, and H.-J. Weyer, Phys. Lett. **112B**, 129 (1982); G. Backenstoss, M. Izycki, M. Steinacher, P. Weber, H.-J. Weyer, K. Von Weymarn, S. Cierjacks, S. Ljungfelt, U. Mankin, T. Petković, G. Schmidt, H. Ullrich, and M. Furić, *ibid.* B **137**, 329 (1984); M. A. Moinster, D. R. Gill, J. Vincent, D. Ashery, S. Levenson, J. Alster, A. Altman, J. Lichenstadt, E. Piasetzky, K. A. Aniol, R. R. Johnson, H. W. Roser, R. Tacik, W. Gyles, B. Barnett, R. J. Sobie, and H. J. Gubler, Phys. Rev. Lett. **52**, 1203 (1984).

[27]J. P. Schiffer, Phys. Rev. Lett. **53**, 736 (1984).

[28]J. W. Negele, Comments Nucl. Phys. **12**, 1 (1983).

[29]A. Nadasen, P. Schwandt, P. P. Singh, W. W. Jacobs, A. D. Bacher, P. T. Debevec, M. D. Kaitchuck, and J. T. Meek, Phys. Rev. C **23**, 1023 (1981).

[30]A. Bohr and B. Mottelson, *Nuclear Structure* (Benjamin, New York, 1969), Vol. I.